Transient Radiative Heating of an Absorbing, Emitting, and Scattering Material

W. W. Yuen* and M. Khatami†
University of California at Santa Barbara, Santa Barbara, California 93106
and
G. R. Cunnington Jr.‡
Lockheed Missiles and Space Company, Inc., Palo Alto, California 94304

The transient heating of a scattering material under direct radiative heating with different back-plate boundary conditions is considered. The radiative transfer is formulated exactly with the one-dimensional solution to the transfer equation. A semiexplicit, fixed-grid, finite-difference technique is used to generate numerical solutions. Numerical results are used to demonstrate parametrically the effect of various radiation parameters on the heating behavior. The transient heating behavior is shown to depend strongly on the optical properties and the assumed thermal conditions at the boundary. For a highly scattering one-dimensional slab with an adiabatic back surface, a temperature "reversal" phenomenon is observed.

Nomenclature

$A(\kappa)$	= coefficient defined by Eq. (20)
$B(\kappa)$	= coefficient defined by Eq. (21)
C_p	= specific heat
$E_n(x)$	= exponential integral function
G	= dimensionless radiative source term, $S/n^2\sigma T_i^4 - (1/\pi)$
h	= enthalpy
h_c	= external heat-transfer coefficient
I	= collimated surface radiative flux
I_0	= collimated incident external flux
J	= diffuse surface radiative flux
K	= extinction coefficient
k	= thermal conductivity
L	= thickness of the one-dimensional slab
n	= index of refraction
q_r	= radiative flux
S	= radiative source term
T	= temperature
t	= time
x	= position coordinate
ϵ_2	= emissivity at the back surface
κ	= optical thickness defined by Eq. (4)
κ_L	= optical thickness of the slab defined by Eq. (5)
λ	= parameter defined by Eq. (9b)
ρ	= density
σ	= Stefan-Boltzmann constant
τ_1	= normal transmissivity at the front surface
$\tau_{1,h}$	= hemispherical transmissivity at the front surface
ω_0	= scattering albedo

Subscripts

1	= front surface
2	= back surface
+	= in the positive x direction
−	= in the negative x direction

Introduction

THE effect of radiative heat transfer in the heating, melting, and ablation of semitransparent materials under direct radiative heating is a problem of considerable importance in the semiconductor and aerospace industries. Typical applications include the processing of multilayer devices or substrate materials in the semiconductor field, the thermal analysis of laser protection shields in the aerospace industries, and the analysis of ice melting with short-wave radiation. Over the years, many analyses have been performed[1-4] to demonstrate the importance of radiation in the thermal performance of various semitransparent materials. Most of these works, however, ignored the scattering effect. For the thermal anlaysis of polycrystalline materials that are known to have large scattering coefficient in the solid phase, the applicability of these results is quite limited.

Of the many thermal analyses developed for heat shield materials available in the literature,[5-9] it is interesting to note that most ignored the effect of radiation. Thus, they are not applicable for the analysis of thermal response of these materials under radiative heating. Howe et al.[7] and Arai[8] included the radiation effect in their analysis of polytetrafluoroethylene (Teflon) heat shields for planetary re-entry applications. A two-flux model, however, was used to formulate the radiation effect. Since the applicability of the two-flux model for a scattering medium is uncertain, their results are ineffective in illustrating quantitatively the importance of scattering on both the transient heating and ablation process. In a related work, Shih et al.[9] analyzed the melting and ablation of Teflon. The heat flux method[10] (which is a modification of the two-flux method) is used to formulate the radiation effect. The effect of scattering, however, was also ignored.

The objective of the current work is to present an accurate mathematical analysis for the transient heating of a one-dimensional absorbing, emitting, and scattering medium. The radiative transfer equation will be solved exactly so that the effect of scattering can be assessed quantitatively. Numerical results will be presented to illustrate the transient heating behavior for this class of materials before melting and abla-

tion. The melting and ablation results (which require the introduction of a two-phase "mushy" zone concept even for a single-component pure substance) will be presented in a later publication.

Mathematical Formulation

A. Energy Equation

The geometry and coordinate system for the present one-dimensional analysis is shown in Fig. 1. Conservation of energy can be written as

$$\rho \frac{\partial h}{\partial t} = \frac{\partial}{\partial x}\left(k \frac{\partial T}{\partial x}\right) - \frac{\partial q_r}{\partial x} \qquad (1)$$

In Eq. (1), ρ is assumed to be constant so that thermal expansion (which must exist if density varies with temperature) and its related effect can be ignored in the present consideration. Over the range of temperature in which this analysis is expected to be applied (say, from 300 to 600 K for Teflon), the density for most heat shielding material varies typically by less than 40% (the reported density of Teflon, for example, changes from 2.17 to 1.44 g/cm^3). Neglecting the density variation thus should not affect significantly the accuracy of the model. Note that enthalpy is used in the heat storage term for these equation because specific heats for these materials generally vary with temperature. Equation (1) can also be readily applied to the melting/ablation problem.

B. Formulation of the Radiative Flux

A generalized formulation of the radiative flux for a material that is nongray and radiatively absorbing and scattering is quite extensive and laborious. To simplify the mathematics, the present work assumes gray medium with temperature-independent optical properties. While these assumptions restrict somewhat the general applicability of the present results, they are reasonable approximations for materials such as Teflon. Results of the present work are thus useful in analyzing the heating behavior of such materials.

For a collimated parallel radiative energy beam with flux density I_0 incidented normally onto the front surface, a diffuse background radiation of σT_i^4, and a diffusely reflecting boundary of constant temperature T_i at the back of the slab, the radiative source term can be written as

$$\frac{\partial q_r}{\partial x} = K[-I_{+s1}e^{-\kappa} - I_{-s2}e^{(\kappa - \kappa L)} - 2J_{+s1}E_2(\kappa)$$

$$-2J_{-s2}E_2(\kappa_L - \kappa) - 2\pi \int_0^{\kappa_L} S(\kappa')E_1(|\kappa - \kappa'|)\, d\kappa'$$

$$+ 4\pi S(\kappa)] \qquad (2)$$

where $S(\kappa)$ is the source function given by solution to the following integral equation

$$S(\kappa) = (1 - \omega_0)\left[\frac{n^2\sigma T^4(\kappa)}{\pi}\right] + \frac{\omega_0}{4\pi}\left[I_{+s1}e^{-\kappa} + I_{-s2}e^{(\kappa - \kappa L)}\right.$$

$$+ 2J_{+s1}E_2(\kappa) + 2J_{-s2}E_2(\kappa_L - \kappa)$$

$$\left. + 2\pi \int_0^{\kappa_L} S(\kappa')E_1(|\kappa - \kappa'|)\, d\kappa'\right] \qquad (3)$$

In the above expressions, the medium is assumed to be dielectric with real index of refraction n. The optical thickness κ is given by

$$\kappa = \int_0^x K(x')\, dx' \qquad (4)$$

with

$$\kappa_L = \int_0^L K(x')\, dx' \qquad (5)$$

Note that K and ω_0 are both functions of position. The medium is assumed to scatter isotropically in the development of Eq. (3).

The parameters I and J stand for collimated and diffuse flux evaluated at the appropriate boundaries. The subscripts " + " and " − " represent flux propagating in the positive x and negative x direction. The various I and J in Eqs. (2) and (3) are shown schematically in Fig. 1.

Their specific expressions are:

$$I_{+s1} = \frac{I_0\tau_1}{1 - (1 - \tau_1)(1 - \epsilon_2)e^{-2\kappa L}} \qquad (6)$$

$$I_{-s2} = \frac{I_0\tau_1(1 - \epsilon_2)e^{-\kappa L}}{1 - (1 - \tau_1)(1 - \epsilon_2)e^{-2\kappa L}} \qquad (7)$$

$$I_{-s1} = \frac{I_0\tau_1(1 - \epsilon_2)e^{-2\kappa L}}{1 - (1 - \tau_1)(1 - \epsilon_2)e^{-2\kappa L}} \qquad (8)$$

$$J_{+s1} = \sigma T_i^4 \tau_{1,h} + (1 - \tau_{1,h})J_{-s1} \qquad (9)$$

$$J_{-s1} = 2J_{-s2}E_3(\kappa_L) + 2\pi \int_0^{\kappa_L} S(\kappa')E_2(\kappa')\, d\kappa' \qquad (10)$$

$$J_{-s2} = (1 - \epsilon_2)J_{+s2} + n^2\epsilon_2\sigma T_L^4 \qquad (11)$$

$$J_{+s2} = 2J_{+s1}E_3(\kappa_L) + 2\pi \int_0^{\kappa_L} S(\kappa')E_2(\kappa_L - \kappa')\, d\kappa' \qquad (12)$$

In terms of the index of refraction, τ_1 can be written as

$$\tau_1 = 1 - \left(\frac{n - 1}{n + 1}\right)^2 \qquad (13)$$

where $\tau_{1,h}$ in terms of n can be obtained from standard references.[11] For simplicity, it is assumed to be the same as τ_1 in the present work.

Equations (9–12) can be further combined to yield

$$\lambda J_{+s1} = \tau_{1,h}\sigma T_i^4 + 2\pi(1 - \tau_{1,h})\int_0^{\kappa_L} S(\kappa')E_2(\kappa')\, d\kappa'$$

$$+ 4\pi(1 - \tau_{1,h})(1 - \epsilon_2)E_3(\kappa_L)\int_0^{\kappa_L} S(\kappa')E_2(\kappa_L - \kappa')\, d\kappa'$$

$$+ 2\epsilon_2(1 - \tau_{1,h}E_3(\kappa_L) \qquad (9a)$$
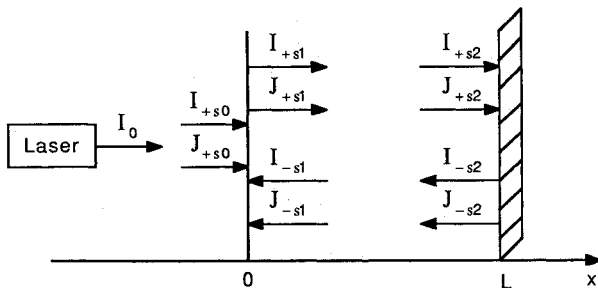

Fig. 1 Geometry, coordinate system, and identification of the various boundary radiative fluxes and their direction.

where

$$\lambda = 1 - 4(1 - \tau_{1,h})(1 - \epsilon_2)E_3^2(\kappa_L) \tag{9b}$$

$$J_{-s2} = 2(1 - \epsilon_2)\left[E_3(\kappa_L)J_{+s1} + \pi \int_0^{\kappa L} S(\kappa')E_2(\kappa_L - \kappa')\, d\kappa' \right]$$

$$+ \epsilon_2 n^2 \sigma T_L^4 \tag{11a}$$

C. Boundary and Initial Conditions

The energy boundary condition at $x = 0$ is given by

$$-\left(k\frac{\partial T}{\partial x} \right)_0 = h_c(T_i - T_0) + I_{+s0} + J_{+s0} \tag{14}$$

with

$$I_{+s0} = \tau_1 I_0 - \tau_1 I_{-s1} \tag{15}$$

$$J_{+s0} = \sigma T_i^4 \tau_{1,h} - \tau_{1,h} J_{-s1} \tag{16}$$

The front surface is heated convectively with a heat-transfer coefficient h_c, and the ambient temperature is assumed to be identical to the initial temperature of the medium T_i.

For highly scattering materials, numerical results show that the radiative and heat transfer boundary condition at the back plate can have significant effects on the transient heating behavior. To illustrate these effects, two different boundary conditions at the back plate will be considered: 1) a reflecting surface at constant temperature T_i, and 2) an insulated surface. For case 1, Eqs. (1–16) are sufficient for a complete mathematical description of the transient heating problem. For case 2, an additional condition at $x = L$ is required. It is

$$I_{+s2} - I_{-s2} + J_{+s2} - J_{-s2} - k\left(\frac{\partial T}{\partial x} \right)_L = 0 \tag{17}$$

In this case, the back-plate temperature T_L is unknown and must be determined as a function of time as part of the solution.

It is important to note that in order to simplify the mathematics and to illustrate more clearly the fundamental effect of radiation, a number of physical effects that might play an important role in the transient heating process are not included in the present analysis. The flow and/or diffusion of the gaseous products of pyrolysis and their effect on the overall heat transfer (convective loss from the solid, attenuation of the incoming radiation flux, etc.), for example, are not considered. The present model is thus somewhat limited in its ability to analyze and correlate actual experimental data. Nevertheless, results of the present analysis are sufficient to demonstrate qualitatively the effect of radiative scattering on general melting/ablation processes.

Method of Solution

Numerical solutions to Eq. (1) are generated by the standard finite-difference fixed-grid formulation with a semiexplicit scheme. Specifically, Eqs. (3), (9a), and (11a) are first combined and the source function $S(\kappa)$ at the $(p + 1)$th time step is

evaluated by

$$\left[S(\kappa) - \frac{\omega_0}{2} \int_0^{\kappa L} S(\kappa')E_1(|\kappa - \kappa'|)\, d\kappa' \right]_{P+1}$$

$$- \left[\frac{\omega_0}{\lambda} A(\kappa)(1 - \tau_{1,h}) \int_0^{\kappa L} S(\kappa')E_2(\kappa')\, d\kappa' \right]_{p+1}$$

$$- \left[\omega_0 B(\kappa) \int_0^{\kappa L} S(\kappa')E_2(\kappa_L - \kappa')\, d\kappa' \right]_{p+1}$$

$$= (1 - \omega_0)\left[\frac{n^2\sigma T^4(\kappa)}{\pi} \right]_p + \frac{\omega_0}{4\pi}\left[I_{+s1}e^{-\kappa} + I_{-s2}e^{(\kappa - \kappa_L)} \right]_p$$

$$+ \left\{ \frac{2A(\kappa)}{\lambda}\left[\tau_{1,h}\sigma T_i^4 + 2\epsilon_2(1 - \tau_{1,h})E_3(\kappa_L) \right] \right.$$

$$\left. + 2\epsilon_2 n^2 \sigma E_2(\kappa_L - \kappa)T_L^4 \right\}_p \tag{18}$$

where

$$A(\kappa) = E_2(\kappa) + 2(1 - \epsilon_2)E_3(\kappa_L)E_2(\kappa_L - \kappa) \tag{19}$$

$$B(\kappa) = (1 - \epsilon_2)\left[\frac{2A(\kappa)}{\lambda}(1 - \tau_{1,h})E_3(\kappa_L) + E_2(\kappa_L - \kappa) \right] \tag{20}$$

The enthalpy is then updated with Eq. (1) with all temperature terms on the right-hand side evaluated at the pth time step and radiative source terms evaluated at the $(p + 1)$th time step. Numerical results show that this scheme is stable numerically and does not require an excessively small time step for a good degree of accuracy. All of the numerical results are generated with a time step of 0.035 s. In a typical calculation (slab thickness of 0.5 cm, reflecting wall with $\epsilon_2 = 0.2$ at the back and constant wall temperature), a reduction of time step to 0.0175 s leads to a variation in the surface temperature by less than 0.08%.

Results and Discussion

To illustrate the general effect of scattering on the heating process, numerical results are generated for highly scattering material with optical properties ($K = 18.06$ cm^{-1}, $\omega_0 = 0.99$) that corresponded approximately to those for Teflon at different wavelengths.[12] Thermophysical properties of Teflon are also used. These properties, which are identical to those used by Arai,[8] are summarized in Table 1. The incident collimated
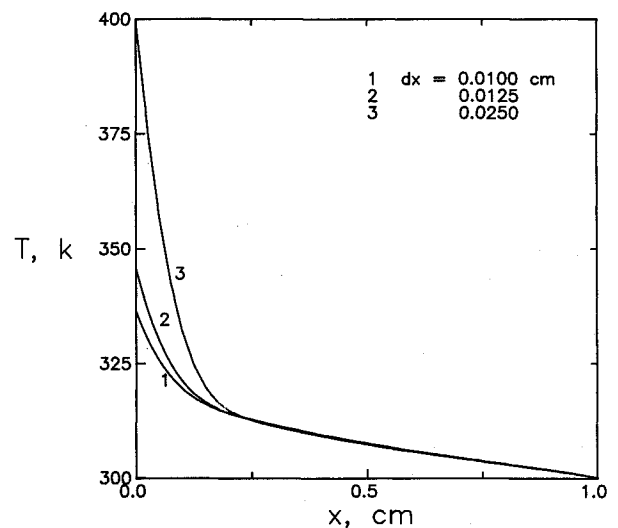
Table 1   Thermophysical properties used in the calculation

Property	Value
k, cal/(cm$-$s$-K$)	$(1.2 + 1.467 \times 10^{-2}T/K) \times 10^{-4}$
C_p, cal/(g$-K$)	$0.123 + 0.373 \times 10^{-3}T/K$
ρ, gm/cm^3	2.167
n	1.36

Fig. 2   Temperature distribution of $t = 4$ s for convergence test on the grid size with $\epsilon_2 = 1.0$.
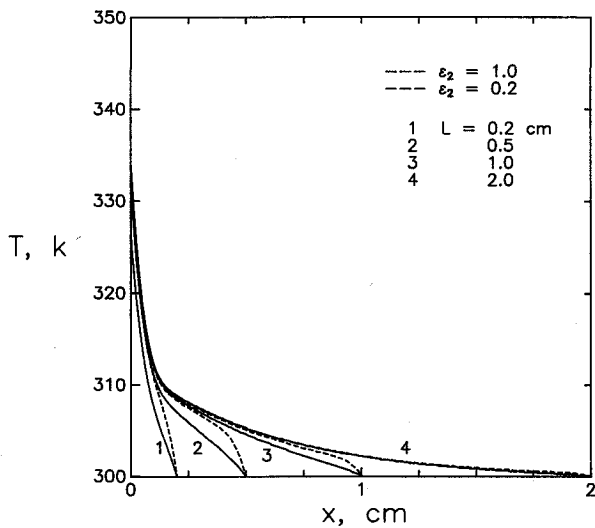
Fig. 3a   Temperature distribution at $t = 2.5$ s for different values of L with $\omega_0 = 0.99$.
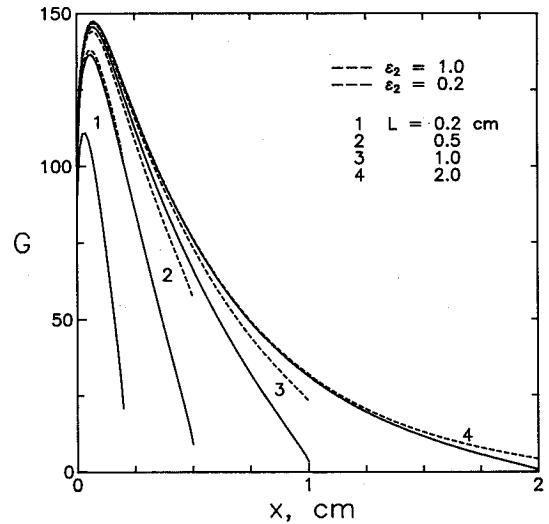

Fig. 3c   Dimensionless source function distribution at $t = 2.5$ s for different values of L with $\omega_0 = 0.99$.
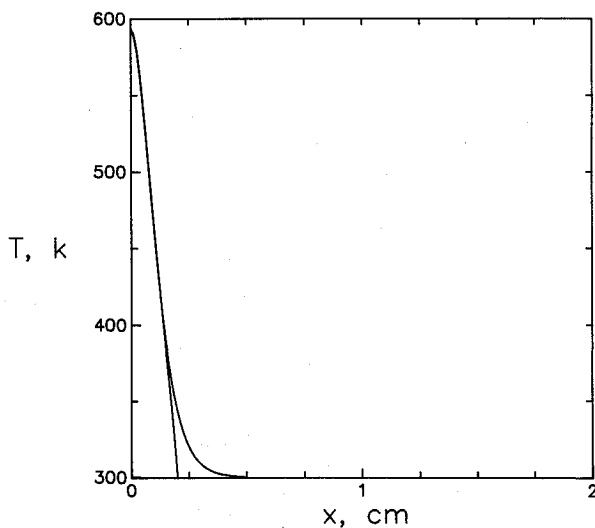

Fig. 3b   Temperature distribution at $t = 2.5$ s for different values of L with $\omega_0 = 0.5$ (note that the temperature distribution is independent of ϵ_2 and is independent of L for $L > 0.5$ cm).
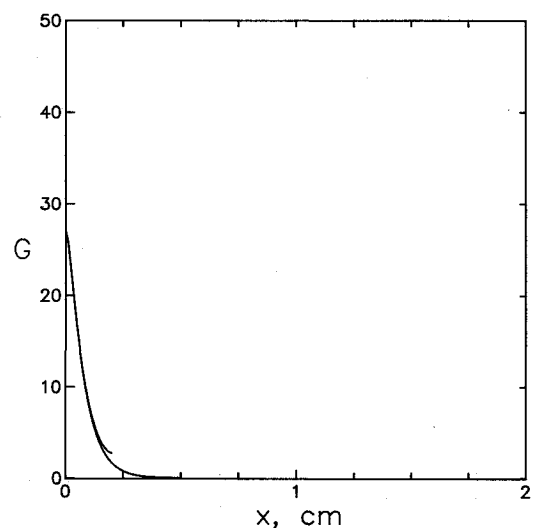

Fig. 3d   Dimensionless source function distribution at $t = 2.5$ s for different values of L with $\omega_0 = 0.5$ (note that the source function distribution is independent of ϵ_2 and is independent of L for $L > 0.5$ cm).

flux is set at 42 W/cm², which corresponded to the power of a CO_2 laser used in some preliminary Teflon ablation experiments performed at Lockheed. To illustrate clearly the effect of radiative heating, the surface heat-transfer coefficient h_c is assumed to be zero in all computations.

As expected, the numerical solution is very sensitive to the grid size. A comparison of results generated by different grid sizes for a typical calculation is shown in Fig. 2. Based on these results, a grid size of 0.0125 cm is selected to generate the remaining results presented in this work.

Discussion of results will be presented in two parts corresponding to different boundary conditions at the back plate.

A.   Reflecting Surface

The temperature distributions calculated for materials with different scattering albedo ($\omega_0 = 0.99$, 0.5) at 2.5 s after the initial heating are shown in Figs. 3a and 3b. The cases shown correspond to slabs of different thicknesses (0.2, 0.5, 1.0, and 2 cm) and different emissivities in the back wall ($\epsilon_2 = 1.0$, 0.2). As expected, the temperature increase in all cases is confined within a thin region near the surface because of the relatively

large optical thickness. The surface temperature increase is higher and the thermal penetration is lower for the case with lower scattering albedo ($\omega_0 = 0.5$) due to the increased absorption. For low emissivity in the back wall ($\epsilon_2 = 0.2$), the temperature distributions in Fig. 3a show an inflection because of the heating of the medium by radiative reflection from the back wall. Scattering has the effect of increasing the penetration of radiative energy into the slab as demonstrated by the corresponding source function distributions shown in Figs. 3c and 3d. Note that for the highly scattering case ($\omega_0 = 0.99$, Figs. 3a and 3c), the source function is dominated by the scattering of the incoming collimated beam. The source function has a maximum at the interior of the medium at which the medium's temperature is not a maximum. For the low-scattering case ($\omega_0 = 0.5$ Figs. 3b and 3d), on the other hand, the source function is dominated by the medium's emission. The source function distribution is qualitatively similar to the temperature distribution, with a maximum at the surface. Because of the increased radiative penetration, the back wall emissivity and the slab thickness both affect the transient heating behavior for the strongly scattering case ($\omega_0 = 0.99$).

Since Teflon is expected to go through a sharp, reversible solid-state phase change at 600 K, the temperature distributions presented in Fig. 3b represent the initial profile before "melting" for the low-scattering case. The corresponding temperature profiles for cases with $\omega_0 = 0.99$ are presented in Fig. 4. For the case with $L = 0.2$ cm, melting fails to occur and the steady-state temperature distribution is shown. A plot of required time to get to the melting temperature after initial heating is presented in Fig. 5. Because of the smaller absorption and longer preheating time, materials with higher scattering albedo appear to have higher average temperature and smaller surface temperature gradient at the beginning of melting. Scattering is thus expected to play a significant role in the subsequent melting behavior. This effect will be illustrated more fully in a future work.

B. Insulated Surface

Since scattering increases the radiative penetration, the boundary condition assumed in the back wall is expected to have important effects on the transient heating behavior. In cases of rapid heating (say, with a high-power laser), an insulated back wall is a more realistic physical assumption. This is the motivation of the numerical results presented in this section.

The temperature distributions at the beginning of melting for cases with an insulating back wall are shown in Figs. 6a and 6b. Both the scattering albedo and the emissivity of the back wall have significant effect on the temperature distribution. In contrast to the previous results, the temperature distributions for the high scattering case are not monotonic. Physically, scattering increases the radiative penetration and temperature of the insulated back wall rises rapidly. The medium near the back wall is subsequently heated by conduction. In general, the minimum of the temperature distribution occurs at the slab's interior while the maximum occurs at either the front or the back surface depending on the slab thickness. For thin slabs ($L < 1.0$ cm), melting begins at the back surface. The time required to reach the melting temperature for the various cases are presented in Table 2.

It is interesting to note that this "temperature reversal" effect has been observed experimentally for other highly scattering materials under radiative heating (e.g., the back-melting of an ice layer heated with short-wave radiation).[3] For heat shielding materials such as Teflon, this effect is expected to have significant implications not only on the material's melting behavior but also on other design considerations such as thermal stress analysis.
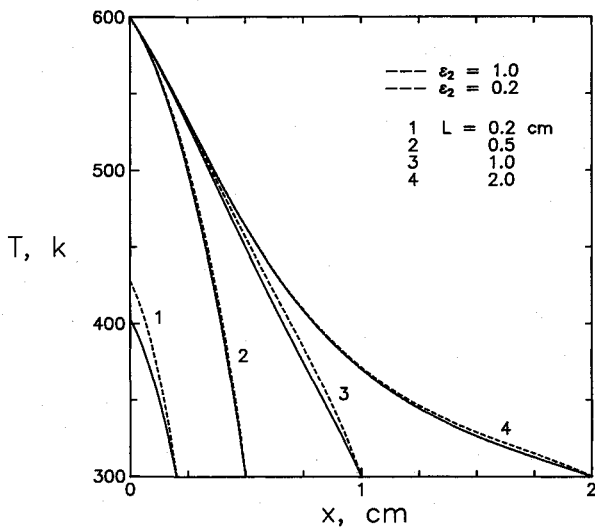

Fig. 4 Solid temperature distribution at the beginning of melt for $\omega_0 = 0.99$.
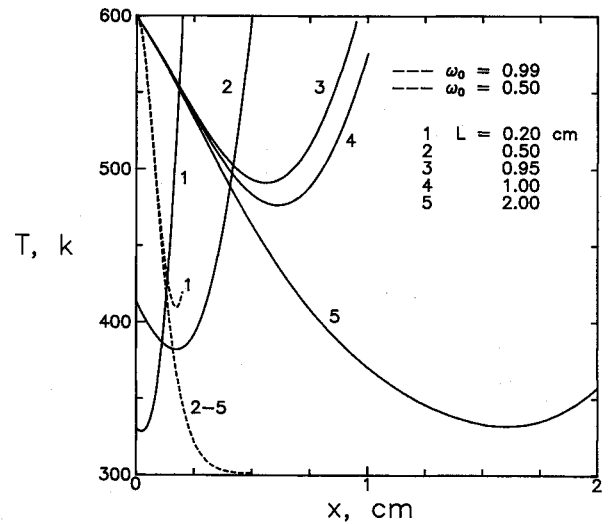

Fig. 6a Solid temperature distribution at the beginning of melt for insulated boundary with $\epsilon_2 = 1.0$.
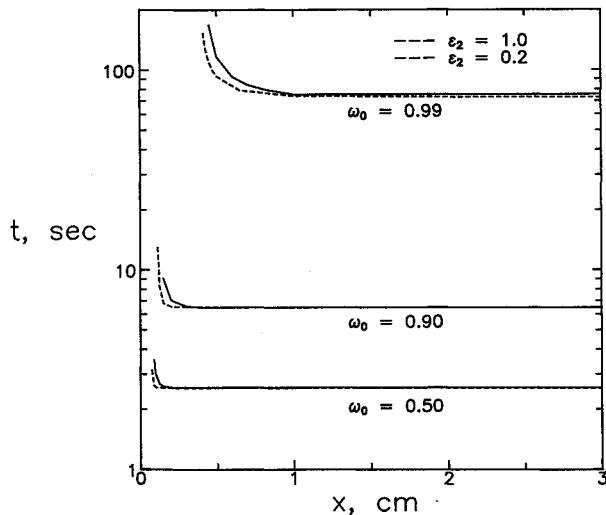

Fig. 5 Time to get to the melting point vs slab thickness for constant back wall temperature.
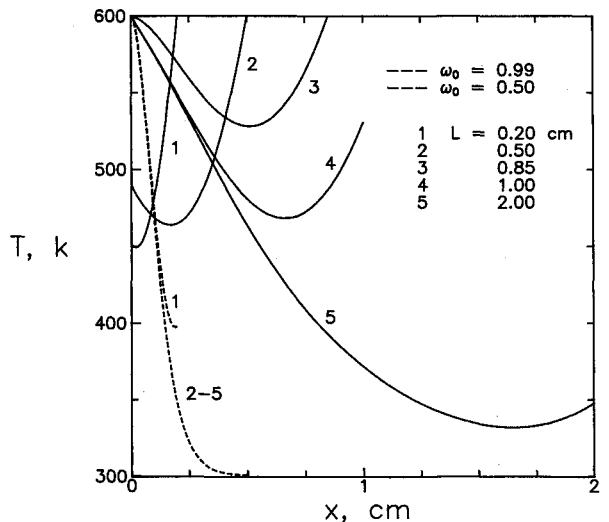

Fig. 6b Solid temperature distribution at the beginning of melt for insulated boundary with $\epsilon_2 = 0.2$.

Table 2 Required time (s) to reach melting temperature for cases with an insulated back surface

	$L = 0.20$ cm		$L = 0.50$ cm	
ω_0	$\epsilon = 0.20$	$\epsilon = 1.0$	$\epsilon = 0.20$	$\epsilon = 1.0$
0.50	2.54	2.56	2.55	2.55
0.90	5.92	5.08	6.45	6.45
0.99	11.23	3.15	31.45	17.06

C. Comments on Comparison with Experimental Data

Some preliminary experiments involving the heating and ablation of Teflon have been performed at Lockheed. Comparison between the prediction from the present model with data, however, is quite difficult. Many experiments, for example, were conducted with Teflon cylinders that were insulated circumferentially. While conductive heat transfer within these cylinders can be readily approximated as one-dimensional, the radiative heat transfer is basically two-dimensional, particularly for material with a large scattering albedo. As shown by results of the one-dimensional problem with an insulated back wall, the reflection and/or absorption by the insulated boundary can have significant effect on the temperature distribution. For a few cases in which the radius-to-thickness ratio is large (so that the one-dimensional assumption might be considered as reasonably valid even for radiation), the sample is heated convectively. It is also important to note that materials such as Teflon are nongray and scattering, if occurring, is often anisotropic. For situations in which the self-emission of the medium is of the same order or large compared to conductive heat transfer and external radiative heating, the present model can be inaccurate.

In short, meaningful comparison between model and experiment requires either additional data for systems in which the radiative transfer can be considered as one-dimensional or an extension of the model to include the two-dimensional effect, convective heat transfer, anisotropic scattering, and the nongray optical properties. Both efforts are currently underway, and results will be presented in future publications.

Conclusions

The transient heating of a one-dimensional solid subjected to radiative heating by a collimated beam is considered. The emphasis of the analysis is to understand parametrically the effect of scattering by the virgin material on the transient heating process. For simplicity, only isotropic scattering is considered.

Numerical results are generated to demonstrate parametri-

cally the effect of various radiative parameters. The conclusions are the following:

1) Scattering increases the long-distance effect of radiative heating. The temperature distribution within a scattering material is not an accurate indicator of the penetration of the incident radiative energy. The radiative source term distribution represents more effectively the region of influence of the incident energy.

2) The temperature distribution of a highly scattering material depends strongly on the assumed thermal conditions on the boundary. For a one-dimensional slab with an insulated back surface under direct radiative heating, a temperature reversal can occur. The minimum of the temperature distribution occurs in the interior with two maxima occurring at the front and back surface. For a thin slab with a large scattering albedo, melting begins at the back surface.

References

[1]Habib, I. S., "Solidification of Semi-Transparent Materials by Conduction and Radiation," *International Journal of Heat and Mass Transfer*, Vol. 14, 1971, pp. 2161–2164.

[2]Abrams, M. and Viskanta, R., "The Effect of Radiative Heat Transfer Upon the Melting and Solidification of Semi-Transparent Crystals," *ASME Journal of Heat Transfer*, Vol. 96, 1974, pp. 184–190.

[3]Seki, N., Sugawara, M., and Fukusako, S., "Back-Melting of a Horizontal Cloudy Ice Layer with Radiative Heating," *ASME Journal of Heat Transfer*, Vol. 101, 1979, pp. 90–95.

[4]Chan, S. H., Cho, D. H., and Kocamustafaogullari, G., "Radiative Transfer with Phase Change—A New Formulation and Solution," American Society of Mechanical Engineers, New York, ASME Paper 80-HT-30, July 1980.

[5]Clark, B. L., "A Parametric Study of the Transient Ablation of Teflon," *ASME Journal of Heat Transfer*, Vol. 94, 1972, pp. 347–354.

[6]Pope, R. B., "Simplified Computer Model for Predicting the Ablation of Teflon," *Journal of Spacecraft and Rockets*, Vol. 12, No. 2, March–April, 1975, pp. 83–88.

[7]Howe, J. T., Green, M. J., and Weston, K. C., "Thermal Shielding by Subliming Volume Reflectors in Convective and Intense Radiative Environments," *AIAA Journal*, Vol. 11, July 1973, pp. 989–994.

[8]Arai, N., "Transient Ablation of Teflon in Intense Radiative and Convective Environment," *AIAA Journal*, Vol. 17, June 1979, pp. 634–640.

[9]Shih, T. M., Hsu, I. C., and Cunnington, G. R., "Combined Conduction and Radiation with Phase Change in Teflon Slabs," *Radiation in Energy System*, edited by T. W. Tong and M. F. Modest, ASME, New York, 1986, pp. 25–31.

[10]Selcuk, N., and Siddall, R. G., "Two-Flux Spherical Harmonic Modeling of Two Dimensional Radiation Transfer in Furnaces," *International Journal of Heat and Mass Transfer*, Vol. 19, 1976, pp. 313–321.

[11]Siegel, R., and Howell, J. R., *Thermal Radiation Heat Transfer*, 2nd ed., McGraw-Hill, New York, 1981.

[12]Based on data obtained at Lockheed.